SAN-1876-2

THIN-FILM POLYCRYSTALLINE SILICON SOLAR CELLS

Quarterly Report No. 2 for December 11, 1978—March 10, 1979

By
Brian W. Faughnan
Joseph Blanc
David Redfield

May 1979

Work Performed Under Contract No. ET-78-C-03-1876

RCA Laboratories
Princeton, New Jersey

U.S. Department of Energy

Solar Energy

SAN-1876-2
Distribution Category UC-63e

THIN-FILM POLYCRYSTALLINE SILICON SOLAR CELLS

B. W. Faughnan
RCA Laboratories
Princeton, New Jersey 08540

MAY 1979

QUARTERLY REPORT NO. 2
For the Period 11 December 1978 to 10 March 1979

Prepared for
Department of Energy
San Francisco Operations
1333 Broadway
Oakland, California 94612

ABSTRACT

In the second quarter, 40 solar cells were fabricated on Wacker substrates. One series of cells was used to compare the effect on AM-1 parameters of making the cells from the center region or the edge region of the original 10x10-cm wafer. Another series tested the effect of varying the junction diffusion temperature from 850 to 900°C. In both cases the differences were not large, except for diffused junctions at 850°C.

Passivation of grain boundaries by heating in a plasma discharge containing atomic hydrogen was attempted on a number of cells. With one ion-implanted cell, which was poor to begin with, a 21% improvement in efficiency was obtained. However, on a number of other more efficient cells, there was no significant improvement.

A variety of experimental techniques for studying polycrystalline silicon and the effects of grain boundaries were implemented this quarter. They include measurement of minority carrier lifetime, QE curves with and without bias light, QE measurements using a 150-μm spot, within a grain and including a grain boundary, laser scans across grain boundaries, and deep-level spectroscopy by transient capacitance. These measurements allowed us to assess the effects of grain boundaries on solar-cell performance.

The surface topography of etched and polished cells was studied by SEM. An SEM method of determining the crystallographic orientation of small grains, called electron channeling patterns (ECP), was developed. The phosphorus diffusion profiles in Wacker material inside a grain and including a grain boundary were measured by SIMS. The presence of small black inclusions in Wacker material was observed.

PREFACE

This Quarterly Report, prepared by RCA Laboratories, Princeton, NJ 08540, describes work performed from 11 December 1978 to 10 March 1979 in the Energy Systems Research Laboratory, B. F Williams, Director. The Project Scientist is B. W. Faughnan and the Project Supervisor is A. H. Firester, Head, Process and Applications.

TABLE OF CONTENTS

LIST OF ILLUSTRATIONS

LIST OF ILLUSTRATIONS (Continued)

LIST OF TABLES

SECTION I

INTRODUCTION

A. DESCRIPTION OF PROJECT

The objectives of this contract, briefly stated, are: to prepare solar-cell structures on Wacker* "Silso" polycrystalline substrates; to establish solar-cell properties of above solar cells; to laser scan the structures to identify regions of degraded response; to characterize electronic and optical properties of above regions; to structurally and chemically characterize grain boundary regions; and to grow bicrystals and boundaries with specific structures and characterize as above.

B. SUMMARY OF WORK THIS QUARTER

1. Preparation and Measurement of Solar Cells on Wacker Polycrystalline Substrates and Single-Crystal Control

Twenty-four completed cells and 21 partially completed cells were prepared this quarter. AM-1 measurments were made on the completed cells, including a group of 6 for an edge versus center of wafer study, 9 for a temperature drive-in study, and 6 which had very poor I-V characteristics and were not used further.

2. Experimental Measurements

In addition to the measurements described above, the following experiments were performed. A group of cells was subjected to atomic hydrogen in a hydrogen glow discharge plasma in an attempt to passivate the grain boundaries. These experiments are described in Section III. The electrical and optical measurements described in Section IV include measurement of minority carrier lifetime by the diode reverse recovery technique, measurement of QE (quantum efficiency) with and without bias light, measurement of QE with a fine spot (150 μm) inside and on grain boundaries, measurement of L_n (minority carrier diffusion length) on a bare unprocessed wafer by the surface photovoltage technique and the measurement of deep traps by the transient capacitance method.

Chemical and structural characterization studies (Section V) included the measurement of surface topography by SEM (scanning electron microscope), obtaining

*Wacker Chemical Corp., Richardson, TX.

electron channeling patterns (ECP) on the SEM which allow determination of the crystallographic orientation of single grains, measurement of phosphorous diffusion profiles in Wacker polycrystalline material by SIMS (secondary ion mass spectroscopy), and the observation of inclusions in polycrystalline silicon.

SECTION II

PREPARATION AND AM-1 MEASUREMENT OF SOLAR CELLS

A. PREPARATION OF SOLAR-CELL STRUCTURES

More than 40 solar-cell structures have been either completed or partially completed in this quarter. A summary of these cells, which also includes the 16 cells completed in the first quarter, is shown in Table 1. We now briefly discuss the cells in that list.

TABLE 1. SUMMARY OF SOLAR CELLS FABRICATED IN FIRST SIX MONTHS OF CONTRACT

Cell No.	Junction	Purpose	Comments
401-408	Diffused	Initial set	Okay
409-416	Diffused	Initial set	Okay
417-424	Implant	Not selected	High $R_{\square}$ ($\sim$400 $\Omega/\square$) poor I-V, faulty implant step
425-433	Implant	Not selected	High $R_{\square}$ ($\sim$400 $\Omega/\square$) poor I-V, faulty implant step
434-439	Diffused	Edge-center study	Okay
440-448	Diffused	Drive-in temp study	Okay
455-457	Diffused	Hydrogenation	Not yet metallized
460-468	Implant	Not selected	$R_{\square}$ = 120-140 $\Omega/\square$ (somewhat high), metallized, ready for device fabrication
469-471	Diffused	Hydrogenation	Not metallized
472-474	Diffused	Not selected	T = 875°C, 10-min drive-in
475-478	Diffused	Not selected	T = 875°C, 40-min drive-in.

The first two series prepared in this quarter, 417-424 and 425-433, had ion-implanted junctions. After the normal drive-in treatment at 850°C, the sheet resistance of both sets of wafers was found to be high. $R_{\square} \sim 400\ \Omega/\square$. The first set was made into completed devices, and the I-V characteristics were found to be very poor. Therefore, those cells were not used in any tests. The second set was re-implanted with another equal dose of phosphorus ions. However, the sheet resistance was still high and nothing further was done with these cells.

The next two series, 434-439 and 440-448, are diffused-junction cells, and the measurements on these cells are described below. Cells 455-457 and 469-471 are not yet metallized. They are reserved for hydrogenation experiments to be performed in the next quarter. The remaining cells, 460-468 (ion-implanted junction) and 472-478 (diffused junction), are being completed and will be ready for experiments in the third quarter.

B. MEASUREMENT OF SOLAR-CELL PARAMETERS

1. Edge versus Center

An examination of a typical Wacker substrate (see Fig. 1, Quarterly Report No. 1 [1]) shows that the first 1 to 2 cm from the edge have a different crystallographic grain structure from the central region. This presumably is related to the way the ingot is cooled during growth. The question arises whether solar cells made from the edge region have different properties from those made using the central region. The series 434-439 was designed to answer this question. These six cells include two single-crystal controls, two solars cells made from the center region (only one 2x2-cm solar cell per 10x10-cm wafer), and two cells made from edge cuts. Actually, for the edge cuts, the 10x10-cm wafer was quartered, and the 2x2-cm solar cell was centered on the resulting 5x5-cm wafer. Therefore, the active cell is only partially made up of edge-region material.

The results of the test are shown in Table 2. The difference between edge and center cut is not great, although η_{ave} is 8% higher for the center cut compared with the edge cut. Since the center cut is very wasteful of material, we shall make all of our future solar cells by first quartering the 10x10-cm wafer unless otherwise specified.

2. Diffusion Drive-in Temperature

Nine diffused junction solar cells were prepared at three different diffusion temperatures, 900, 875, and 850°C. In each case the $POCl_3$ gas flowed for 15 min and was followed by a 25-min drive-in at the same temperature. Three cells were prepared at each temperature: single-crystal control, Wacker etched

1. B. W. Faughnan, Thin-Film Polycrystalline Silicon Solar Cells, Quarterly Report No. 1, prepared under Contract No. ET78-C-03-1876 for Department of Energy, January 1979.

TABLE 2. SOLAR-CELL PARAMETERS AS A FUNCTION OF CENTER VERSUS EDGE CUT ON WACKER 10x10-cm WAFERS

Sample No.	Type	Sheet ρ (Ω/□)	J_{sc} (mA/cm^2)	V_{oc} (mV)	FF	η(no AR) (%)	η(ave) (%)
434C	Control	41.1	21.6	532	0.78	8.9	8.5
435C	Control	56.8	20.8	535	0.72	8.1	
436	Edge	70.9	19.1	522	0.74	7.4	6.9
437	Edge	57.3	18.8	518	0.66	6.4	
438	Center	48.2	19.4	530	0.75	7.7	7.5
439	Center	54.0	19.2	525	0.73	7.4	

surface, and Wacker polished surface. The I-V parameters of the diffused cells described above were measured and are given in Table 3.

The cells whose junctions were diffused at 875°C have solar-cell parameters very similar to cells 401 to 408 [1] whose junctions were formed at the same temperature. The 900°C junctions were not very different. However, there is a big difference between the control and the Wacker cells for the 850°C run. The control cell follows the same general pattern, i.e., J_{sc} rises as diffusion temperature drops whereas V_{oc} varies in the opposite way. The net result is that the efficiency varies only slightly from 850 to 900°C. However, the Wacker cells made at 850°C are very poor. There was some indication from earlier work done at RCA on Wacker substrates that diffusion is not very effective at 850°C or below. Further work is planned to check the possibility that diffusion in Wacker polycrystalline material is slower than in single-crystal silicon.

TABLE 3. SOLAR-CELL PARAMETERS AS A FUNCTION OF JUNCTION DIFFUSION TEMPERATURE

Sample No. & Type	Diff Temp (°C)	Sheet ρ (Ω/□)	J_{sc} (mA/cm^2)	V_{oc} (mV)	FF	η (no AR) (%)
440C	900	18.0	21.5	559	0.77	9.2
441E	900	20.1	20.3	532	0.76	8.3
442P	900	19.1	20.0	537	0.76	8.1
443C	875	51.6	21.7	546	0.77	9.1
444E	875	44.4	19.4	528	0.76	8.0
445P	875	37.7	19.1	515	0.75	7.4
446C	850	149	21.9	530	0.76	8.8
447E	850	212	5.2	146	0.48	0.4
448P	850	220	17.2	348	0.43	2.6

SECTION III

PASSIVATION OF GRAIN BOUNDARIES - HYDROGENATION EXPERIMENTS

A. INITIAL EXPERIMENTS ON TWO WACKER SOLAR CELLS

In this quarter we initiated some experiments on the passivation of grain boundaries of completed solar cells fabricated on Wacker polycrystalline substrates by heating them in a glow discharge containing atomic hydrogen. Recently such treatment has been found to greatly reduce the surface conductivity of certain polycrystalline silicon samples [2], although the effect on solar cells was not investigated.

This is similar to the treatment which can significantly affect the performance of amorphous silicon solar cells and may lead to the removal of dangling bonds. Two solar cells were treated, one (415) with an ion-implanted junction and very poor characteristics, the other (402) with a diffused junction and good characteristics. The change in solar-cell parameters is listed in Table 4. The I-V curves for cell 415 are shown in Fig. 1. The poorest cell showed the largest improvement, 21% in the efficiency. In a better cell J_{sc} did not change but there was an improvement in V_{oc} and FF. The quantum efficiency of cell 415 was remeasured and found to improve after hydrogenation.

B. MORE DETAILED STUDIES ON FIVE SOLAR CELLS

The initial experiments described above were encouraging. Therefore we performed a new series of tests on five solar cells:

401C	Diffused junction, single-crystal control
403	Diffused junction, Wacker
413C	Ion-implant junction, single-crystal control
414	Ion-implant junction, Wacker
415	Ion-implant junction, Wacker

Three different treatments were tried: (1) 300°C, 1 h, in H (plasma discharge); (2) 500°C, 15 min, in He (heat treatment typically used to obtain good ohmic contacts of the Ti-Ag fingers); and (3) 425°C, 8 h, in H (plasma discharge).

The results are shown in Table 5. First consider the two control samples. The ion-implant sample (413C) shows virtually no change throughout the three

2. C. H. Seager and D. S. Ginley, Appl. Phys. Lett. 34, 337 (1979).

TABLE 4. EFFECT OF HYDROGENATION ON SOLAR-CELL PARAMETERS OF TWO WACKER CELLS

Cell No.	Junction Type	Treatment	J_{sc}/mA before/after	V_{oc} (mV) before/after	FF before/after	η^*(%) before/after
415	Ion implanted	300°C, 1 h in H	17.3/18.9	460/499	0.66/0.68	5.3/6.4
402	Diffused	325°C, 3 h in H	19.8/19.8	535/541	0.71/0.78	7.5/8.3

*No AR coating, AM-1 simulation.

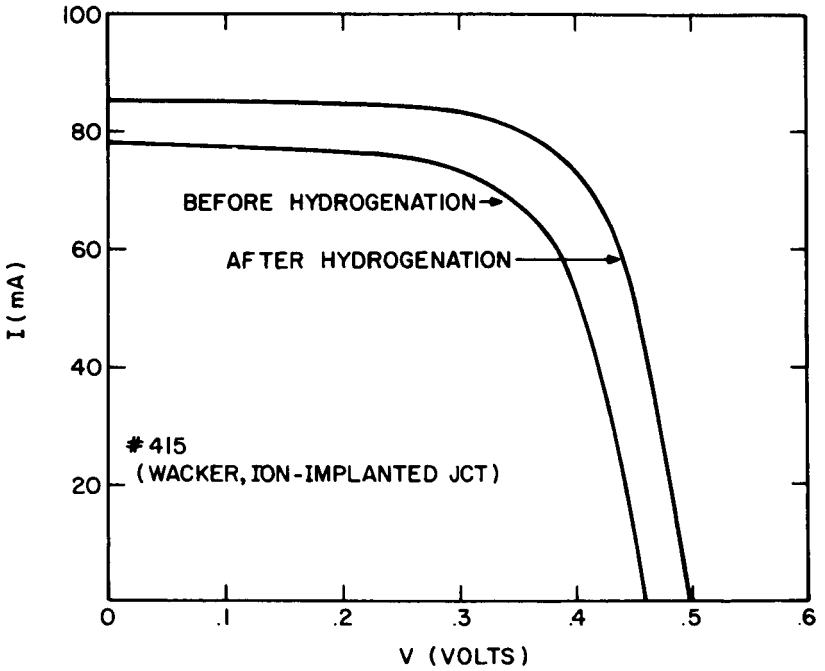

Figure 1. Light I-V curve of solar cell 415 (Wacker, ion-implanted junction) before and after hydrogenation for 1 h at 300°C.

treatments. The diffused junction cell (401C) shows small variations but the net effect of the three treatments is nil. This is the expected result since these cells have no grain boundaries which can be affected. Next, consider the diffused junction Wacker cell 403. This shows an improvement of 5% in the efficiency after the first treatment but this is primarily due to an improvement in the fill factor. Only small changes occur after the next two treatments and the net effect is a 3% improvement in efficiency due mainly to the improved fill factor. This improved fill factor is probably just a temperature effect (improved metallization contact resistance) rather than a result of the hydrogenation.

Finally we consider the two Wacker ion-implanted cells. Primarily, these show degradation with each heat treatment except for the first treatment on cell 415, which shows an improvement. This cell had been subjected to two earlier hydrogenation treatments, 300°C for 1 h and 325°C for 3 h. The first of these improved the efficiency by 21%, the second treatment decreased η by 6%, and the first of the present treatments (300°C, 1 h) increased η by 5%. All subsequent treatments decrease η. The final result is that 414 and 415 have decreased in efficiency by 15 and 20%, respectively.

TABLE 5. SUMMARY OF HYDROGENATION EXPERIMENTS ON FIVE WACKER CELLS

	Treatment:	300°C, 1 h in H			500°C, 15 min in He		425°C, 8 h in H		
	Meas. Date:	2/1/79	1/5/79		2/15/79		2/20/79		Total
	Sample No.	Before	After	%Δ	After	%Δ	After	%Δ	%Δ
401C	J_{sc} (mA/cm^2)	22.9	22.2	-3.0	21.9	-1.5	22.6	+3.5	-1.4
	V_{oc} (mV)	562	560	-0.4	560	0	561	+0.2	-0.2
	FF	0.78	0.79	+1.0	0.78	-1.2	0.79	+1.2	+1.2
	η(%)	10.04	9.84	-1.6	9.57	-2.7	10.02	+4.5	0.0
403	J_{sc}	19.7	19.6	-0.5	19.3	-1.5	19.2	-0.5	-2.5
	V_{oc}	530	528	-0.4	530	+0.4	533	+0.5	+0.6
	FF	0.72	0.77	+7.0	0.76	-1.3	0.76	0	+5.6
	η	7.53	7.93	+5.0	7.77	-2.0	7.78	0	+3.3
413C	J_{sc}	19.6	19.6	0	19.6	0	19.6	0	0
	V_{oc}	519	520	0.2	521	0.2	520	0.2	+0.2
	FF	0.76	0.76	0	0.76	0	0.76	0	0
	η	7.73	7.73	0	7.73	0	7.73	0	0.0
414	J_{sc}	19.5	19.2	-1.5	19.5	+1.5	19.4	-0.5	-0.5
	V_{oc}	509	502	-1.4	501	+0.2	471	-6.0	-7.0
	FF	0.70	0.69	-1.4	0.67	-3.0	0.66	-1.5	-5.7
	η	6.93	6.73	-3.0	6.55	-2.7	6.03	-7.9	-15.0
415	J_{sc}	18.9	19.0	+0.5	19.3	+1.5	18.2	-5.5	-4.0
	V_{oc}	483	490	+1.4	492	+0.4	445	-9.5	-10.0
	FF	0.67	0.69	+3.0	0.67	-3.0	0.60	-9.0	-10.0
	η	6.13	6.43	+4.8	6.36	-1.1	4.86	23.6	-20.7

To summarize the results so far, we have obtained one good result, namely, cell 415, which was initially anomalously low in efficiency, was improved by 25% with a single hydrogenation experiment. On the other Wacker samples, hydrogenation had a small effect or led to degradation of solar-cell parameters. One possible problem is that hydrogenation was carried out on completed metallized cells and some of the metal may diffuse down the grain boundaries during heat treatment.

SECTION IV

ELECTRICAL AND OPTICAL MEASUREMENTS OF POLYCRYSTALLINE SILICON

A. MEASUREMENT OF MINORITY CARRIER LIFETIME

We have measured the minority carrier lifetime in the base region in a number of Wacker and control solar cells. The lifetime data can be compared with the diffusion length data obtained from the quantum efficiency (QE) curves by means of the equation $L = \sqrt{D\tau}$ where L is the minority carrier diffusion length; D is the diffusion constant $\sim$ 25 cm^2/s for 6-Ω-cm p-type material; and τ is the minority carrier lifetime.

In Table 6, we list the results for the cells studied. The diffusion lengths as derived from the measured lifetimes are given along with the value derived from the quantum efficiency measurement. The lifetime measurements are carried out on a series of diagnostic dots on either side of the active solar-cell region. These dots vary in diameter from 0.100 to 0.30 in. and are labeled R or L (right or left side of active solar cell), "a" through "d," respectively.

Several observations may be made about these data. For the two control cells, the agreement between the lifetime measurements and the QE measurements is very good. However, for the Wacker cells the lifetime measurements predict a higher diffusion length. For the diffused cell, the measurements predict a diffusion length 50% higher on the average than the optically derived diffusion length, whereas for the implanted cells the diffusion length is approximately ten times higher than the quantum efficiency value. In fact, the diffusion lengths are similar for all Wacker cells as well as the ion-implanted control. On the other hand, the QE curves for the Wacker ion-implanted cells were distinctly inferior to the Wacker diffused cells and could not be fit to the single solar-cell model as explained in the first quarterly report. It appears that the minority carrier lifetime measurement is not sensitive to grain boundaries or bulk traps whereas the QE measurement is. We plan to investigate whether higher carrier injection levels could explain this result.

TABLE 6. DIFFUSION LENGTHS IN WACKER AND CONTROL SOLAR CELLS AS MEASURED BY DIODE REVERSE RECOVERY AND QUANTUM EFFICIENCY CURVES

	Meas. Method	Sample Number 401C	403P	413C	414D	415P
	τRR					
	L a	200	90	85	62	77
(left	b	211	90	85	52	88
side	c	187	71	85	52	50
dots)	d	159	97	--	74	85
	R a	206	75	87	87	81
(right	b	200	72	80	80	57
side	c	151	61	68	68	78
dots)	d	135	63	68	68	79
	QE	250	50	80	6-20	2-8

Cell 401C - control single crystal, diffused junction
403P - Wacker, polished surface, diffused junction
413C - control single crystal, ion-implant junction
414D - Wacker, polished surface, ion-implant junction
415P - Wacker, polished surface, ion-implant junction

B. QUANTUM EFFICIENCY MEASUREMENTS WITH AND WITHOUT DC LIGHT BIAS

In view of the large minority carrier diffusion lengths calculated from the diode reverse recovery measurements, we decided to measure QE with a dc bias light on the cell. Since the QE measurement uses chopped light (550 Hz), the dc bias should not affect the signal except insofar as it changes the minority carrier lifetime of the chopped-light-generated carriers. This could happen, for example, if the dc-light-generated carriers saturated the traps and recombination sites which normally limit the lifetime of the chopped-light carriers. These recombination sites could be at grain boundaries or in the bulk material.

The experiments were tried for two cells which had greatly different L_n values without dc bias light, namely, cells 403 and 415. The results for cell 403 are shown in Fig. 2. Cell 403 is a diffused-junction cell which had L_n = 50 μm without bias light. As bias light from an ELH lamp was applied with increasing intensity, the QE curve increased and saturated at the level shown in Fig. 2. Although the light intensity was not measured, we believe it was approximately 40% of AM-1 intensity. A model fit to this new curve gives L_n = 70 μm, in good agreement with the minority carrier lifetime measurement.

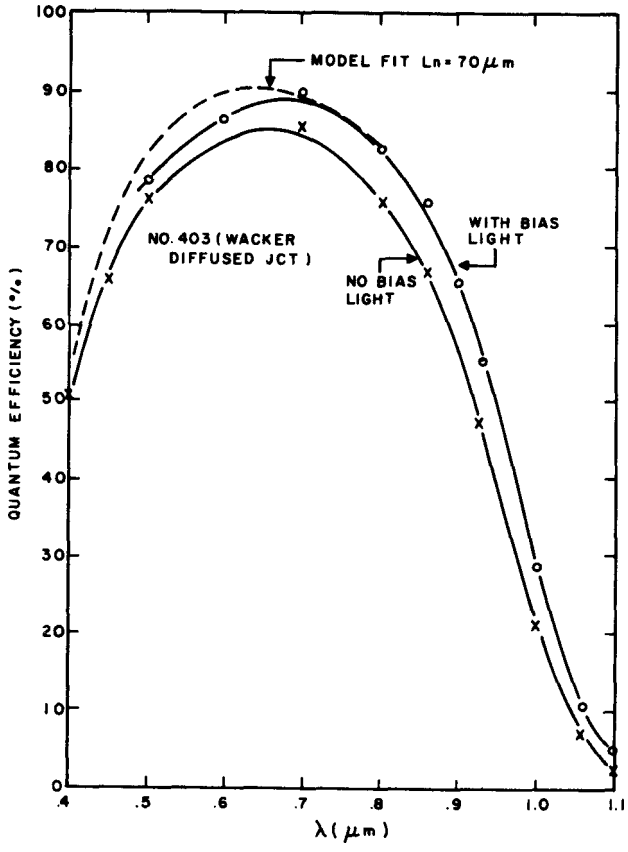

Figure 2. QE curves of solar cell 403 (Wacker, diffused junction) with and without dc bias light.

The effect for cell 415 is even more surprising. This cell had a poor QE to begin with, but it is greatly improved when bias light strikes the cell. In fact for the same light intensity as was used for cell 403, the QE curve obtained is shown in Fig. 3. It is almost identical to cell 403 and also yields L_n = 70 μm, again in agreement with the minority carrier lifetime measurements for that cell. These new values of L_n are actually more consistent with AM-1 solar-cell parameters. For example, from the last column of Table 5, J_{sc} (403) = 19.2 mA/cm^2, J_{sc} (415) = 18.2. These two numbers are not too different, in agreement with the light-bias QE curves, but in disagreement with the dark QE curves.

C. QUANTUM EFFICIENCY MEASUREMENTS WITH 150-μm LIGHT SPOT - WITH AND WITHOUT A GRAIN BOUNDARY

1. Description of Apparatus

For the proper analysis of grain boundary effects, it would be desirable to measure QE with a very fine spot. Then we could measure QE inside a grain well

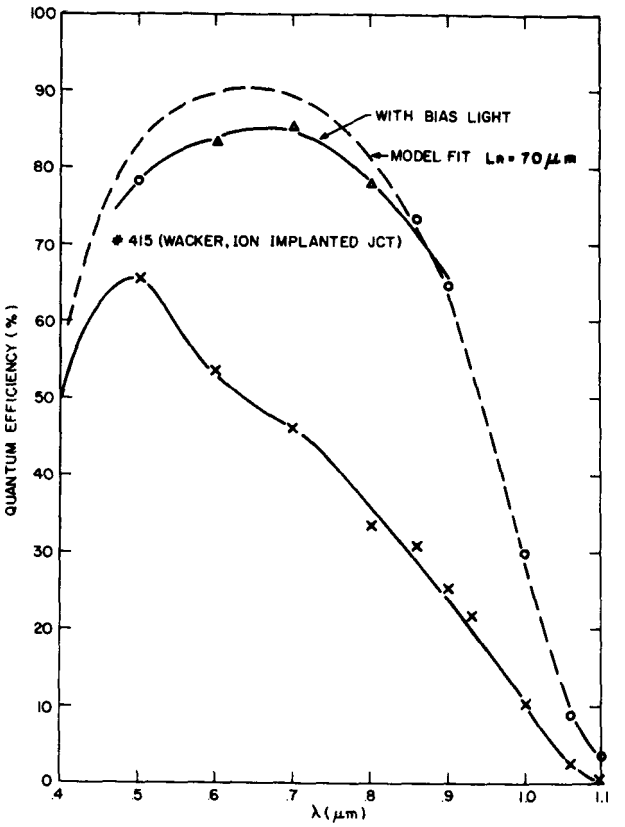

Figure 3. QE curves of solar cell 415 (Wacker, ion-implanted junction) with and without dc bias light.

away from any grain boundaries. Furthermore, if this spot intercepts a grain boundary, the effect of that boundary will be maximized since the total area is small and no illuminated point will be far from the boundary. This is a more difficult problem than the laser scanning case, where only one wavelength is required and a laser can be used. It is relatively easy to achieve diffraction limited optics with the laser, and more difficult with the white light source required for the QE measurement. Nevertheless we were able to achieve a 150-μm spot, which appears to be adequate to do the job.

A schematic diagram of the apparatus is shown in Fig. 4. Many of the optical components of our previous QE apparatus are used here. The new feature is the use of two Tropel collimators. These devices accept a small beam of light (1 to 2 mm) and expand it to a 25-cm beam of collimated light. The second collimator further improves the degree of collimation. The exiting light is parallel to better than 1 degree. The price paid is the loss of most of the light emitted from the lamp. However, sensitivity appears adequate

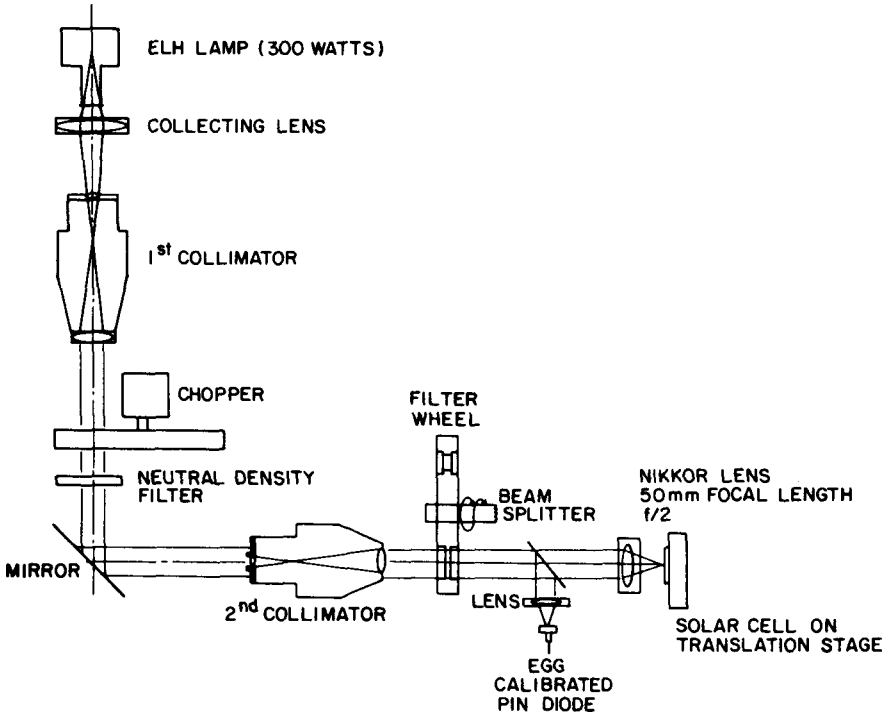

Figure 4. Schematic diagram of the five light spot (150-μm-diameter) QE apparatus.

using chopped light and a phase-sensitive detector. The actual spot size of 150 μm is determined experimentally by sweeping the light spot across a single-crystal solar cell and measuring the decrease in light as the spot is swept across the metal fingers.

2. Experimental Results

Scans of the above light spot across four different solar cells are shown in Fig. 5. The first scan of cell 401C, is a single-crystal control. The only features observed are the dips in signal when the light spot crosses the metal fingers. The next sweep shows cell 403 which is a diffused-junction cell on Wacker polycrystalline material. Here new features are seen as the light spot crosses grain boundaries. Finally the last two cells, 414 and 415, which have ion-implanted junctions, have even more irregular features.

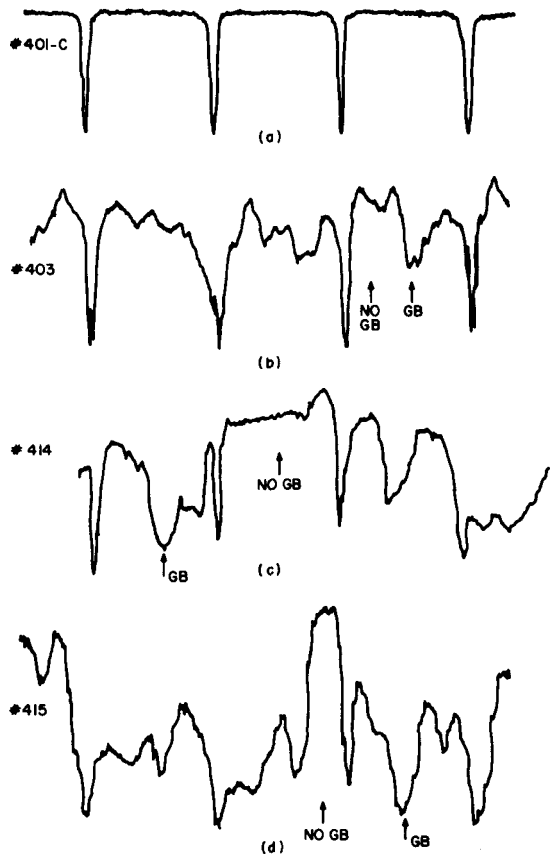

Figure 5. Four light spot scans (150-μm spot) across four solar cells showing effect of metal fingers and grain boundaries on photoresponse.

Figure 6 shows the QE curve obtained for cell 401C. This is virtually identical to the curve obtained last quarter with the 1x8-mm light spot. This is the expected result since this cell has no grain boundaries.

Figure 7 shows QE curves obtained on cell 403. The best curve was obtained in a region with no grain boundaries and yields a minority carrier diffusion length L_n = 50 μm. This is also the value we obtained last quarter with the 1x8-mm light spot. The other two curves are obtained when the light spot intercepts a grain boundary. If the curves are analysed for L_n, effective diffusion lengths of 20 and 30 μm are obtained. Clearly the grain boundary is having a measurable effect.

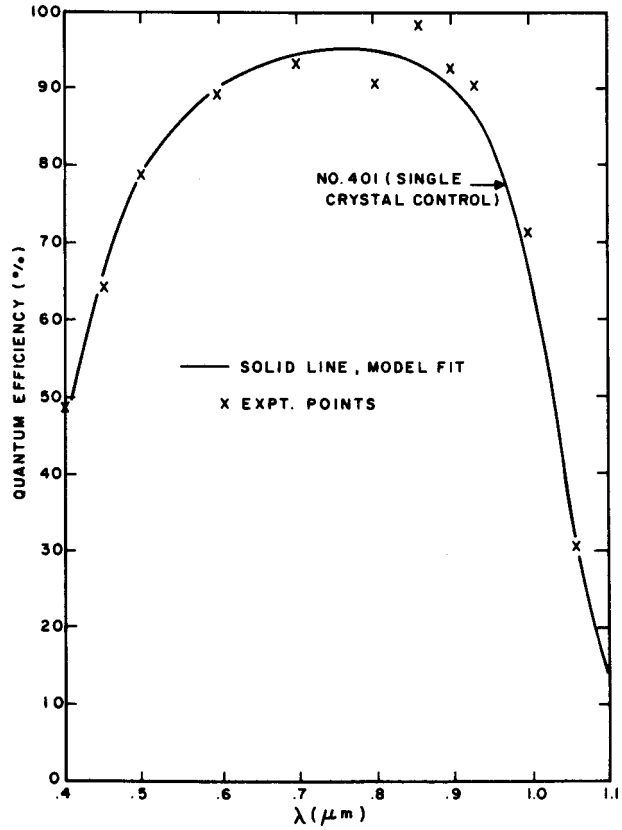

Figure 6. QE curve with 150-μm light spot of solar cell 401C (single crystal control). X_j = 0.5 μm, W = 0, h = 280 μm, L_p = 0.45 μm, L_n = 250 μm, S_p/D_p = 5, S_n/D_n = 0.

The QE curves for the next cell, 414 (ion-implanted junction), shown in .g. 8, are more dramatic. First L_n within the grain is found to be 50 μm, in ;reement with cell 403 (diffused junction), but not in agreement with the QE ırve obtained for this cell last quarter with the 1x8-mm light spot [1]. Apparently ıe grain boundaries have a greater effect in the ion-implanted-junction cell. ıis is supported by the second QE curve of Fig. 8, taken on a grain boundary, ıich gives an effective L_n of 12 μm.

Finally, Fig. 9 shows the results for cell 415 (ion-implanted junction). :re we show two curves taken inside grains, one curve taken across a grain)undary and one curve using a 1.5-cm-diameter light spot which should give ı average value. All the points lie on the same curve and give $L_n \sim 1.6$ μm, ıe lowest value we have yet measured. Apparently the diffusion length in the ılk of this material is so small that the effect of grain boundaries cannot

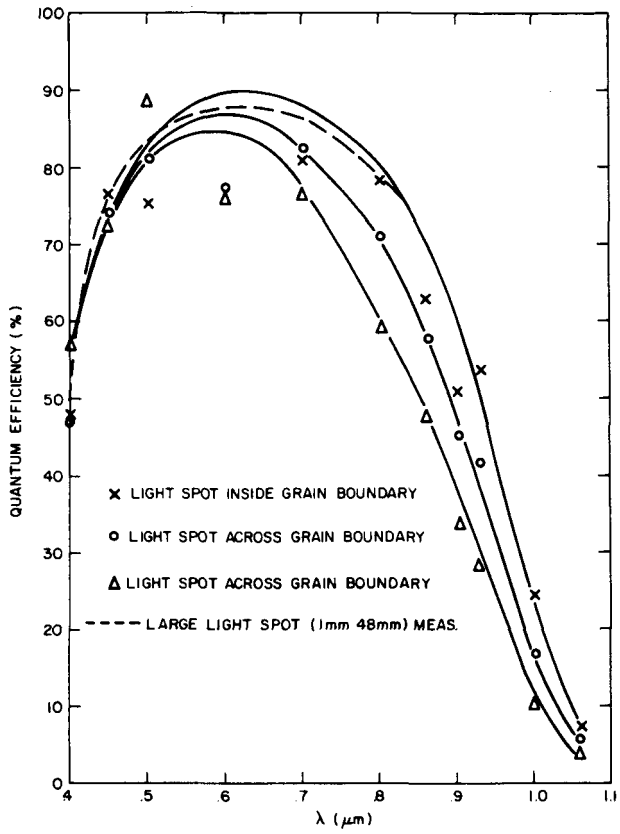

Figure 7. QE curves of cell 403 (Wacker, diffused junction) with 150-μm light spot. X_j = 0.4 μm, W = 0, h = 350 μm, L_p = 0.45 μm, L_n = 20, 30, 50 μm, S_p/D_p = 5, S_n/D_n = 0.

even be observed. This cell has been subjected to a variety of heat treatments as outlined elsewhere in this report, and apparently one or more of these treatments has had a deleterious effect on the base diffusion length, at least at low carrier levels (i.e., no dc light bias).

D. MINORITY CARRIER DIFFUSION LENGTH ON WACKER UNPROCESSED WAFER

The minority carrier diffusion length, L_n, in an unprocessed bare Wacker wafer was measured by the surface photovoltage technique (measured by Ed Douglas). The result for one wafer only was L_n = 5 μm. This low value is consistent with the range of L_n we inferred from QE measurements on ion-implanted cells which have a lower processing temperature than the diffused cells.

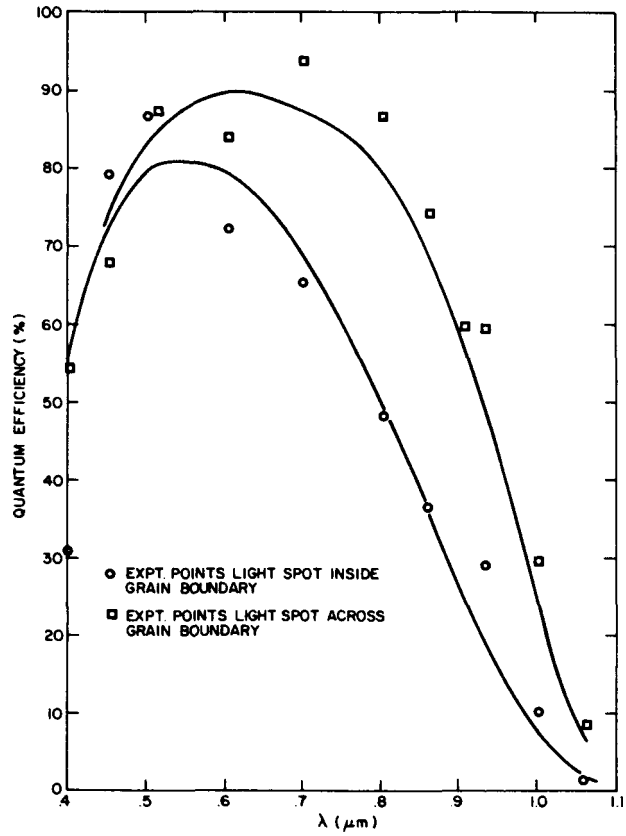

Figure 8. QE curves of cell 414 (Wacker, ion-implanted junction) with 150-μm light spot. Solid lines indicate model fit. X_j = 0.4 μm, W = 0, h = 350 μm, L_p = 0.45 μm, L_n = 12.50 μm, S_p/D_p = 5, S_n/D_n = 0.

E. DEEP-LEVEL SPECTROSCOPY

The goal of this portion of the program is to measure the properties of electrically active deep levels that can be associated with the grain boundaries in polycrystalline silicon and that may be responsible for limiting solar-cell performance. All the deep-level measurements were made with a transient capacitance technique that is now becoming well known. Samples for these measurements are small (~1 mm) mesa diodes formed either on the polycrystalline silicon wafers containing solar cells or on other wafers whose junctions are formed in just the same way. Dark I-V curves are always obtained on the diodes before deep-level measurements. These curves have shown invariably poor ("soft") reverse breakdown characteristics (at 5 to 10 V) on all tested diodes, even those formed on a good single-crystal control wafer (413) having an ion-implanted junction.

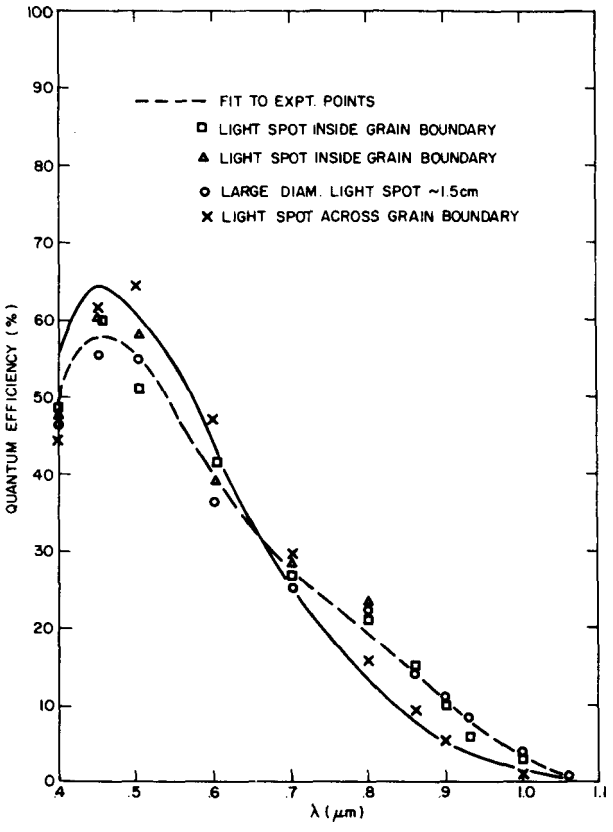

Figure 9. QE curves of cell 415 (Wacker, ion-implanted junction) with 150-μm light spot. Dashed line indicates average fit to experimental points; solid line indicates model fit. X_j = 0.4 μm, W = 0, h = 350 μm, L_p = 1.6 μm, L_n = 1.6 μm, S_p/D_p = 5, S_n/D_n = 0.

To date, deep-level measurements have been made on wafers 411 (implanted Wacker Silso), 406 (diffused Wacker), 413 (implanted single-crystal control) with and without hydrogenation, and 453 (a sample of Wacker Silso selected for very large grains and given a diffused junction). Figure 10 shows the deep-level curves for both 411 and 406 to exhibit the principal features in a comparative way. In neither case is there any sign of the fairly narrow symmetrical peaks that characterize discrete levels in normal silicon. Furthermore, the broad bands that are evident here are very different for implanted and diffused junctions. It is essential, therefore, to determine when we may be observing only the effects of ion implantation so they can be separated from grain-boundary effects. With this goal in mind, similar measurements were made on wafer 413, the implanted single-crystal control. The results are shown in Fig. 11 for which the gain was 10 times as high as for Fig. 10.

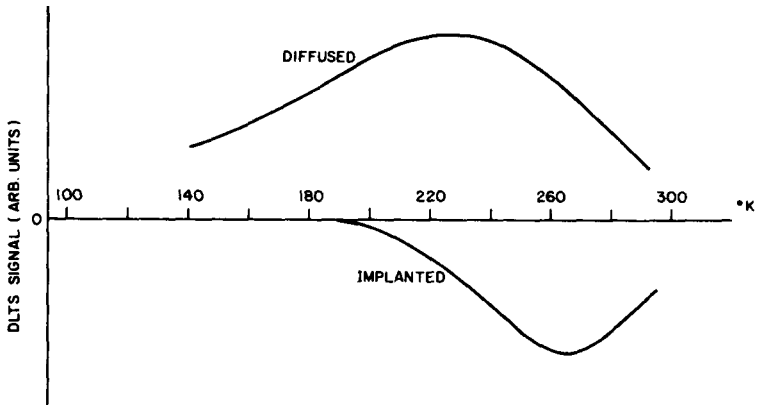

Figure 10. Deep-level spectra (by transient capacitance) of cells 411 (Wacker, ion-implanted junction) and 406 (Wacker, diffused junction).

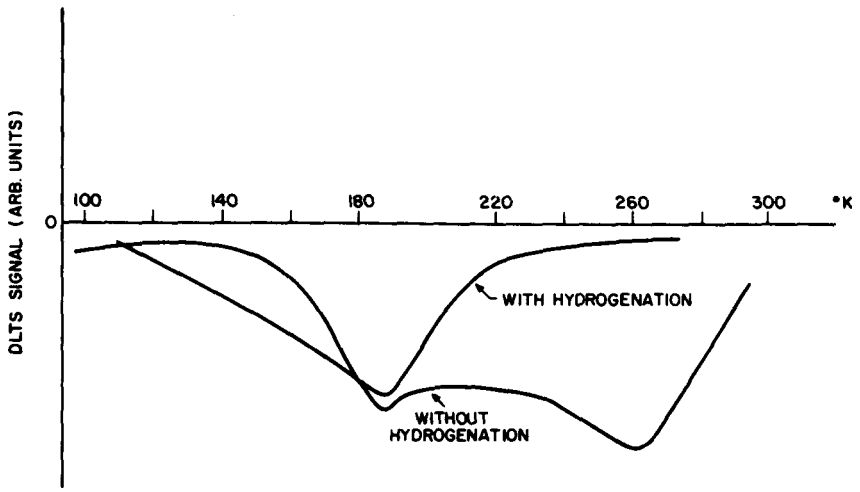

Figure 11. Deep-level spectra (by transient capacitance) of cell 413C (single-crystal control). R diode on right hand side of solar cell, L diode on left hand side.

These results provide the following tentative picture. First, there are deep levels attributable to implantation alone in all of our implanted material, even after annealing. Next, the signals observed in implanted samples are negative, a result that should not occur in this experiment and one for which we are still seeking an explanation. It appears, however, that implantation is interfering with our effort to identify grain-boundary effects. Last, the effect of hydrogenation on control sample 413 is surprisingly prominent in that one of the two bands of deep levels seems to disappear. This result has not yet been reconfirmed because of our emphasis on effects in polycrystalline silicon, but it remains a provocative effect.

A series of samples has been prepared from Wacker wafer 453 which contains some very large (~1 cm) grains in addition to the usual small ones (~1 mm). A junction was diffused in the normal manner to approximately 0.5-μm depth, and the entire 5-cm square was processed into 1-mm-diameter mesa diodes. Photomicrographs show that some diodes have no visible grain boundaries, stacking faults or twins, whereas others have 1 or 2 such defects and still others have the usual several defects. Figure 12 illustrates some of the better diodes.

This series is to be studied for correlations between the physically observable defects, normal electrical properties, and deep-level spectra. In one of these diodes, 453-F8, we have made the first observation of a single, almost normal, deep-level peak, shown in Fig. 13. This supports our view of the prospects for a range of responses.

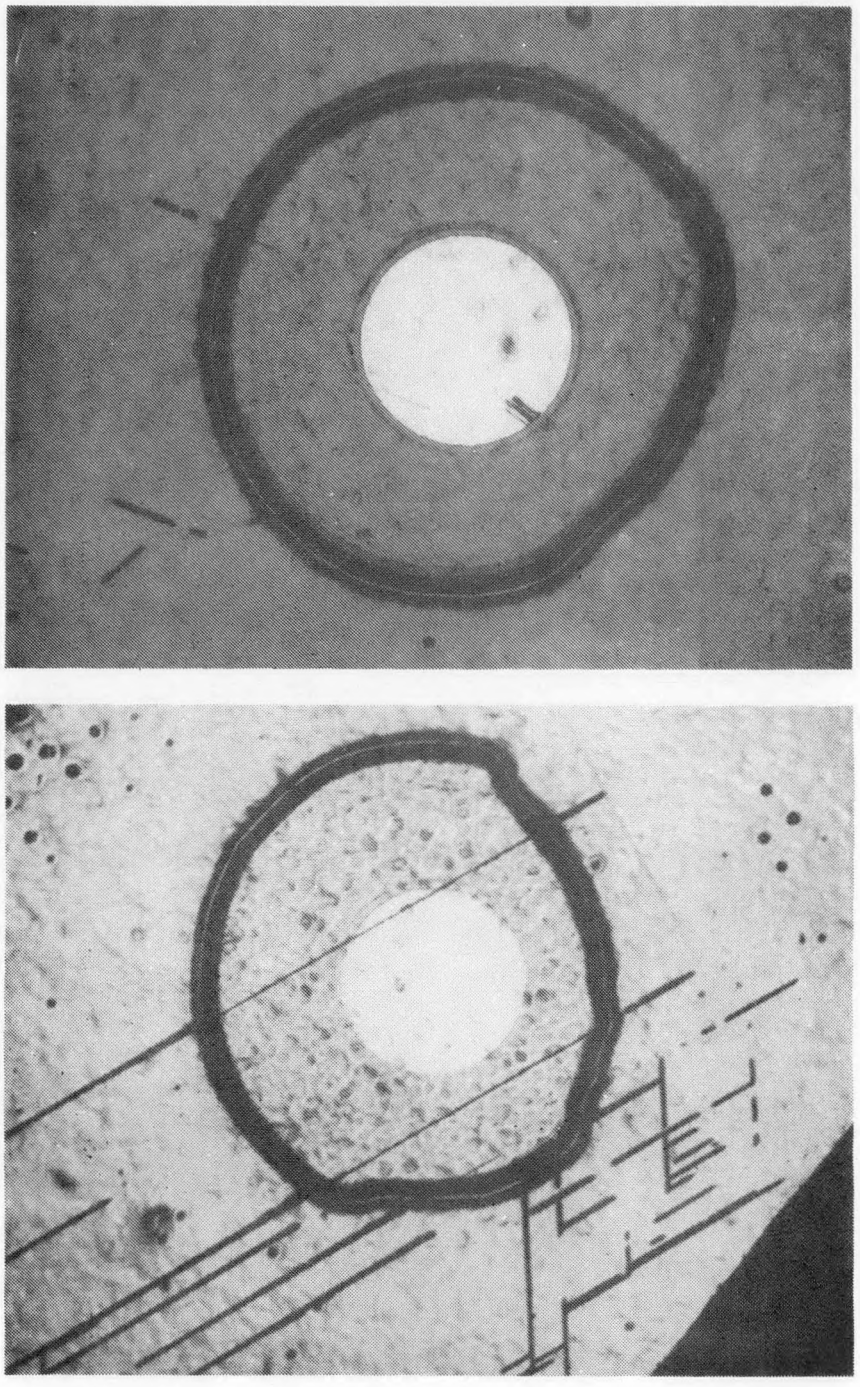

Figure 12. Photographs of diode dots F7 and E7 of wafer 453 (Wacker, diffused junction).

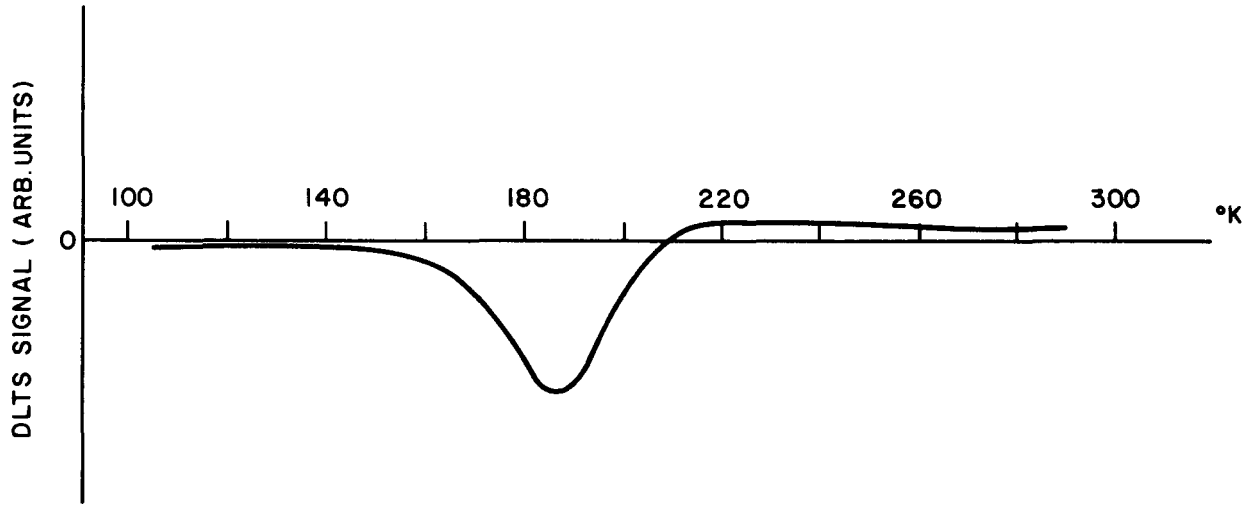

Figure 13. Deep-level spectra of diode dot F8 of wafer 453.

SECTION V

CHEMICAL AND STRUCTURAL CHARACTERIZATION OF POLYCRYSTALLINE SILICON

A. SURFACE TOPOGRAPHY

1. Introduction

The surface roughness of our solar cells is an important parameter not only for understanding the observed photovoltaic characteristics but also for the design and interpretation of auxiliary experiments. We have therefore undertaken a small series of optical microscopic, scanning electron microscopic (SEM), and Talysurf observations to characterize surfaces prepared by our standard methods.

2. Polished Surfaces

These surfaces are prepared by a conventional chemi-mechanical polishing procedure used for single-crystal silicon. To the eye, such surfaces appear highly specular with an occasional faint contrast feature. It is, in fact, difficult to observe the grain boundaries by optical microscopy under arbitrary illumination conditions, but normal illumination yields reasonable contrast at grain boundaries. An example of a low (12.5X) magnification optical micrograph of a polished cell is shown in Fig. 14. The grains within the cells can be clearly seen, although the contrast is much weaker than in the surrounding etched back material. The metallization stripes can also be seen; the regions marked B and C will be discussed below in connection with phosphorus profiles. Talysurf measurements show that different grains differ in height by perhaps as much as 0.2 μm. Unfortunately, all topographical contrast is lost in scanning electron microscopy, probably because the "sidewalls" of the grains have very shallow slopes. We believe that these results can be understood on the assumptions that the mechanical component of the polishing polishes all grains at roughly the same rate, while the chemical component etches grains preferentially, so that the end result is a steady-state difference in elevation between different grains. We do not, however, intend to pursue this matter.

3. Etched Surfaces

These surfaces, observed by eye, have a matte finish. As already seen in Fig. 14, grain boundaries can easily be observed by optical microscopy. They can also be seen by scanning electron microscopy. A nearly cross-sectional SEM

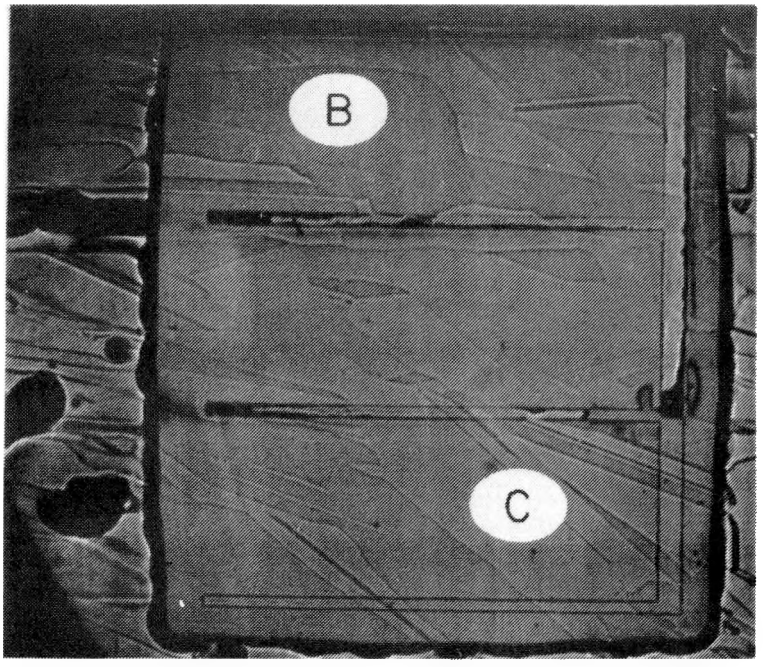

Figure 14. Low magnification optical photograph of a polished surface of Wacker material.

view (85°) is shown in Fig. 15 at a magnification of 2000X. The surface is highly textured with high mountains and low valleys. Both SEM and Talysurf determinations show peak to valley differences of 1 μm or more, although as can be seen in Fig. 15, some grains do etch to a relatively flat surface. Unfortunately, the generally rough surface texture gives rise to very poor electron channeling patterns (see below). This texture should also give rise to very nonuniform boundary conditions for impurity diffusion, especially if the diffusion depth is of the order or smaller than the dimensions of surface roughness as is true here. Fortunately, such effects seem not to have a profound effect on solar-cell characteristics.

B. ELECTRON CHANNELING PATTERNS

The laser scan maps reported in Quarterly Report No. 1 clearly show that some grain boundaries exhibit degraded photoresponse (presumably because of high recombination velocity at the boundary) and some grain boundaries do not. In order to understand the underlying physical reasons for the different behaviors observed, it is clearly necessary to identify, at the very least, the orientation of two grains with respect to each other and to attempt to ascertain what crystallographic planes the boundaries are composed of. The desired results are easy to

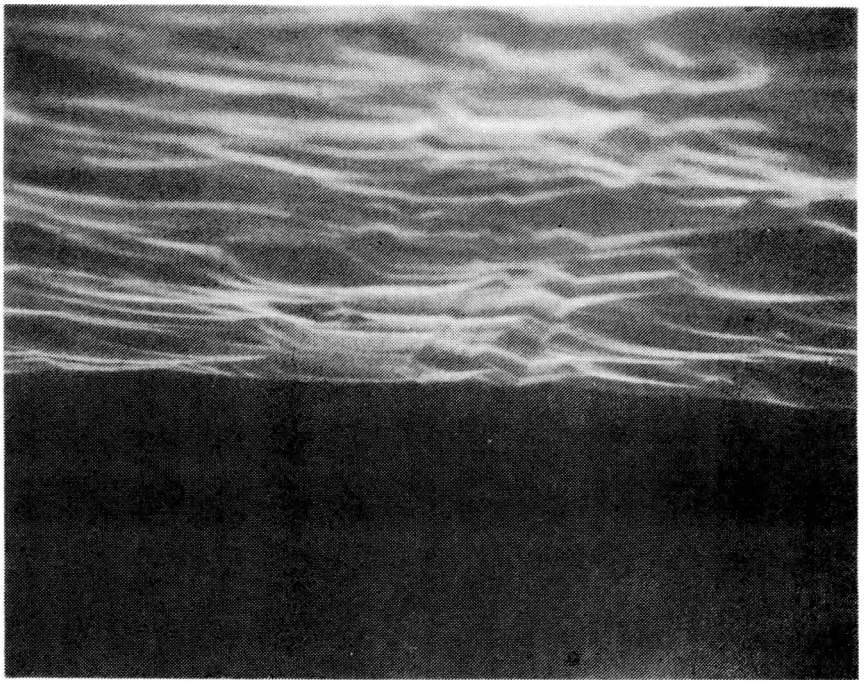

Figure 15. SEM photograph of an etched surface of Wacker material.

describe, but not so easy to obtain. After obtaining an optical micrograph and a laser scan to see which boundaries are "active" and which "inactive," we want to be able to identify grain orientations over an entire solar cell, or a substantial fraction of it. Ideally, we want a method which requires no additional preparation of the specimen and, because of the volume of data to be generated on a single cell, which yields the desired data relatively quickly. The well-known methods for determining crystal orientations (have diffraction, x-ray topography, or transmission electron microscopy) are undesirable for one or several of the following reasons: absence of an image corresponding to the diffracting grain, long data acquisition times for a single orientation, long and tedious specimen preparation, or inability to scan over large areas. Of the methods known to us, only electron channeling patterns from selected areas (SA ECPs) seem capable in principle of handling this problem.

Since ECP is a relatively new technique and one which is used relatively infrequently, we present a very brief background to the subject. The interested reader may wish to consult Booker's review [3]. ECPs were first reported 12 years

3. G. R. Booker, in Modern Diffraction and Imaging Techniques in Material Science, edited by S. Amelinckx, R. Gevers, G. Remaut, and J. Van Landuyt (North-Holland, Amsterdam, 1970) pp. 613-654.

ago by Coates [4]. Under appropriate conditions in the SEM, a set of complex bands can be observed as shown in Fig. 16, which look exactly like Kikuchi bands familiar from transmission electron microscopy. Like Kikuchi bands, these can be used to determine the crystallographic orientation of the specimen surface with respect to the incident electron beam. Soon after Coates' original observations, techniques were developed for selected areas; here the electron beam is restricted to a small area and the beam is rocked about this fixed area.

The details of the contrast-inducing mechanism are quite complex, but a broad physical understanding can be obtained from the Bloch functions of band theory. The wave function of a high-energy electron (in practice larger than 3 keV) in the crystal can be described as a superposition of two types of Bloch waves: one has maxima along atom planes, the other between atom planes. The actual composition of the electron wave depends on its direction of propagation, therefore depending on the angle between the specimen surface and the incident electron beam. Scattered electrons, primary and secondary, which are observed in SEM preserve a partial "memory" and this results in the SA ECP observed as the beam is rocked.

RCA Laboratories did not have the ability to obtain SA ECPs on our SEM instruments. With the active collaboration of E. R. Levin of RCA Laboratories, we completed the necessary modifications and testing. We estimate that an upper limit for the size of the electron probe is ~50 μm, which is ample for our purposes. The probe size is probably significantly smaller than this, and we will investigate this further in the future.

Figure 16 illustrates the type of results we hope to obtain. Figure 16(a) shows a conventional SEM image of an etched sample whose local topography is unusually smooth; a number of grains can clearly be seen. Figure 16(b) and (c) show the SA ECPs of the two points about 200 μm apart indicated as B and C in Fig. 16(a). The ECPs are clearly different, showing that the faint topographic contrast line in the image is indeed a grain boundary. Since these results are only a trial run with no correlation to laser scans, we have not done the crystallographic analysis. As previously mentioned, the general roughness of etched surfaces precludes obtaining satisfactory ECPs from most portions of such surfaces, while polished surfaces give very satisfactory ECPs but not grain boundary contrast. We are now in the course of studying conditions under which previously polished surfaces are lightly etched back to just reveal the grain boundaries in the SEM without introducing intolerable general surface roughening. We are con-

4. D. G. Coates, Philos. Mag. 16, 1179 (1962).

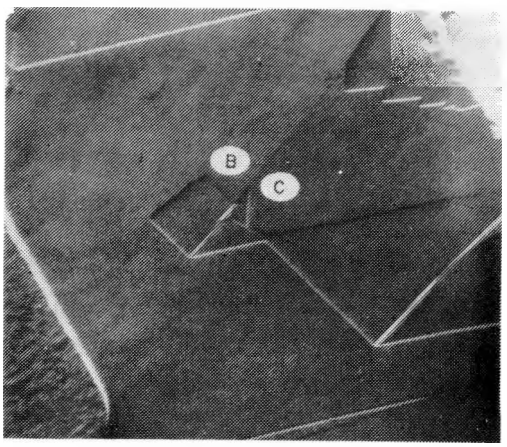

(a)

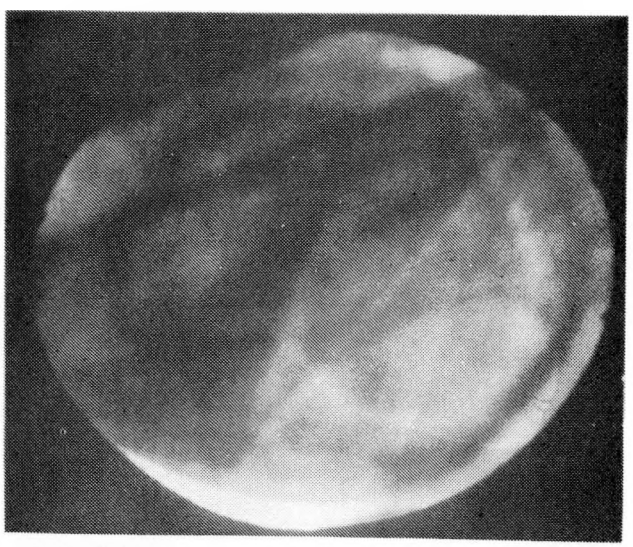

(b)

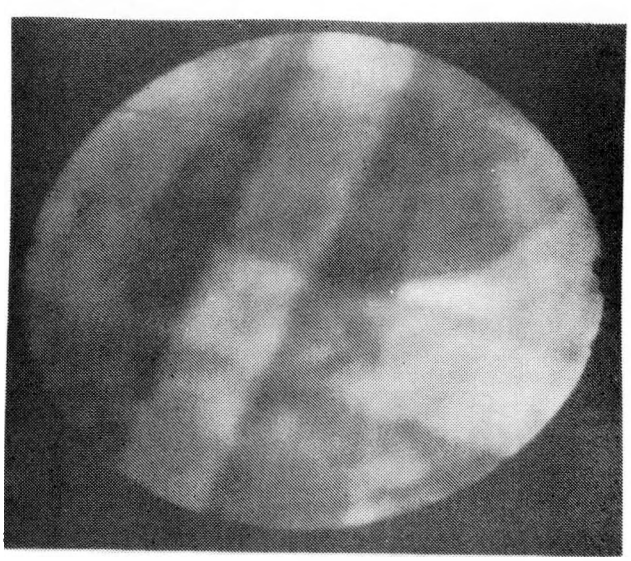

(c)

Figure 16. (a) SEM photograph of Wacker substrate showing regions B and C. (b) Electron channeling patterns taken in region B. (c) Electron channeling patterns taken in region C.

fident that we will find an optimum set of etching conditions without undue effort and soon be able to obtain the desired crystallographic orientations.

C. PHOSPHORUS DIFFUSION PROFILES

For proper detailed modeling of the p-n junctions in our solar cells, it is clearly desirable to have some quantitative measure of phosphorus concentration as a function of distance both in depth from the surface and across grain boundaries. The diffusion of P in single-crystal silicon at the very high surface concentrations used here is already an extremely complicated phenomenon [5], and it is by no means evident what might be expected for phosphorus diffusion either in a single crystal, in polycrystalline silicon, or down a grain boundary.

C. W. Magee of our laboratories has developed a method (using Cs coverage) for the sensitive ($\sim 10^{16}/cm^3$) detection of phosphorus by secondary ion mass spectrometry (SIMS) over areas 250x250 μm, while simultaneously sputtering the specimens. Using this SIMS technique, we have been able to obtain P profiles as a function of depth both in a single grain and in a region containing several grain boundaries. The results are shown in Fig. 17, where the points labelled "single large grain" were obtained from the area labelled B in Fig. 14, while the "grain boundaries" points come from area C. While the spatial resolution is far too poor to rule out rapid diffusion along the boundaries, the data shown in Fig. 17 are more than sufficient to be able to conclude that rapid diffusion and anomalously high concentrations along the boundaries are not occuring simultaneously. Furthermore, there is a small but systematic and real difference between the two curves shown in Fig. 17: for a given depth below the surface, the P concentration is always smaller in the region containing grain boundaries than in the single grain. This result is consistent with data obtained prior to the current contract indicating that, under given P diffusion conditions, the mean penetration of P is systematically less in polycrystalline silicon than in single-crystal silicon. We have begun attempts at modeling these interesting phenomena, but it is far too premature to speculate on their origins.

D. INCLUSIONS IN POLYCRYSTALLINE SILICON

As a side result of the SIMS analysis discussed above, we observed "black specks" in the sputter craters. These proved to be particles typically of 3 to

5. R. B. Fair, J. Appl. Phys. 50, 860 (1979).

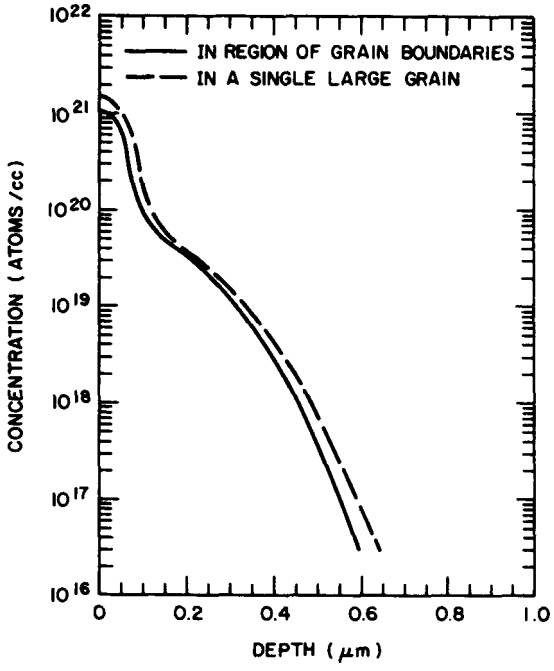

Figure 17. Phosphorus diffusion profile in Wacker polycrystalline silicon.

20 μm, some of which are beautifully crystallographic. An x-ray dispersive analysis carried out in the SEM showed only the presence of silicon in these particles (note that in spite of very high concentration of P, we have found no evidence of silicon phosphide precipitation). This presumably means that the particles contain an element lighter than Na. Of the possible candidates, SiC so far appears to be the most likely; we will attempt to check this by scanning Auger analysis although this will be a difficult experiment. We are in the process of ascertaining whether these inclusions exist in all our wafers or whether the present observation is an isolated incident.

SECTION VI

ANALYSIS OF RESULTS AND SUMMARY

We have established a variety of experimental techniques for studying polycrystalline silicon and the effects of grain boundaries. These include AM-1 measurements, minority carrier lifetime, QE curves with and without bias light, QE measurements using a 150-μm light spot, within a grain and including a grain boundary, minority carrier diffusion length in unprocessed substrates by surface photovoltage technique, laser scans across grain boundaries, passivation of grain boundaries, and deep-level spectroscopy by transient capacitance. In addition chemical and structural techniques have been developed to determine the properties of individual grains.

What have we learned so far by applying these techniques to Wacker polycrystalline material? First of all, AM-1 measurements may not be a sensitive method of studying grain boundaries in this material. This is partly a result of the large average grain size. Of course, we could turn this statement around and say that is why good solar cells can be made from Wacker material and it does not matter how bad the grain boundaries are since there are relatively few of them. This could also mean that grain boundary passivation has only a small effect on the AM-1 parameters of solar cells made from this material.

Nevertheless, we are interested in general techniques which will be sensitive to grain boundary effects. For example, QE measurements with light bias give results in good agreement with J_{sc} measured under AM-1 conditions on the same cell. However, QE measurements in the dark are much more sensitive to material purity and grain boundaries, and showed a marked difference between diffused and implanted cells in the 401-416 series. Similarly the 150-μm light spot QE measurements readily show grain boundary effects.

The difference between L_n obtained from QE inside a grain (150-μm spot) and with dc light bias, i.e., 50 and 70 μm, respectively, implies that the Wacker material has recombination sites in the bulk which saturate at high light level. When an average QE is measured on a diffused-junction cell, with a large light spot, the same value of L_n is obtained, i.e., 50 μm. This implies that the grain boundaries are not very active in diffused-junction cells. Their

effect can be seen, however, with QE measurements using a 150-μm light spot which includes a grain boundary.

The ion-implant cells behave differently. When QE is measured inside a grain, L_n = 50 μm is obtained. This says that the intragrain Wacker material is the same for diffused and implanted cells, a not unexpected result. However, when an average QE is obtained using a large light spot, a much lower L_n results, implying that now grain boundaries are effective in reducing the average L_n. But if dc light bias is applied, this difference disappears, implying that the grain boundary recombination sites are saturated at the higher carrier densities, thereby reducing the difference between the AM-1 parameters of diffused and implanted cells.

Thus we have some indication that diffused junction cells have more passivated grain boundaries than ion-implanted cells. Presumably, this is because phosphorus can diffuse down grain boundaries during drive-in of the junction, but cannot do so to any appreciable extent in the annealing step of ion-implanted cells.

All of these facts must be kept in mind when assessing the effect of various grain boundary passivation treatments of complete solar cells. It would be helpful to look to the more grain-boundary sensitive experiments (e.g., laser scanning and QE with the 150-μm light spot) to assess grain boundary passivation experiments, and we intend to do this in our hydrogenation experiments in the next quarter.

The above discussion of grain boundary effects in Wacker material is not meant to be rigorous, since it is based on only a few experiments. We will use this picture as a guide for future experiments and hope to verify this model with additional experimental results.

SECTION VII

PLANNED FUTURE ACTIVITIES

In the next quarter we plan to set up our 1.15-μm laser scanning apparatus and study photoresponse across grain boundaries in great detail. We hope to obtain a quantitative measure of grain boundary effects, i.e., a surface recombination velocity. We plan to perform more hydrogenation experiments where the effects of atomic hydrogen on grain boundaries will be carefully studied.

Finally we would like to combine the structural characterization (electron channeling patterns) of adjacent grains with laser scans across their common grain boundary.

REFERENCES

1. B. W. Faughnan, Thin-Film Polycrystalline Silicon Solar Cells, Quarterly Report No. 1, prepared under Contract No. ET78-C-03-1876 for Department of Energy, January 1979.

2. C. H. Seager and D. S. Ginley, Appl Phys. Lett. 34, 337 (1979).

3. G. R. Booker, in Modern Diffraction and Imaging Techniques in Material Science, edited by S. Amelinckx, R. Gevers, G. Remaut, and J. Van Landuyt (North-Holland, Amsterdam, 1970) pp. 613-654.

4. D. G. Coates, Philos. Mag. 16, 1179 (1962).

5. R. B. Fair, J. Appl. Phys. 50, 860 (1979).

☆U.S. GOVERNMENT PRINTING OFFICE: 1979-640-258-1535